PERGAMON

Journal of Quantitative Spectroscopy & Radiative Transfer 83 (2004) 629–639

Journal of Quantitative Spectroscopy & Radiative Transfer

www.elsevier.com/locate/jqsrt

Dipole model of spherical hydrometeors and its application on the space-borne precipitation radar sounding☆

Xin Jin[a,*], Li Zhenglong[a], Zhu Yuanjing[a], Wang Zhenhui[b]

[a] *Department of Atmospheric Sciences, School of Physics, Peking University, Beijing 100871, China*
[b] *Department of Electronic Information and Applied Physics, Nanjing Institute of Meteorology, Nanjing 210044, China*

Received 19 September 2002; received in revised form 21 December 2002; accepted 27 February 2003

Abstract

To study the characteristics of spherical hydrometeors influenced by Ku-band precipitation radar, the exact expressions of scattering cross-section, $Q^{(s)}$, back scattering cross-section, $Q^{(b)}$, absorption cross-section, $Q^{(a)}$, and attenuation cross-section, $Q^{(e)}$, of small spherical precipitation particles are deducted according to the assumption of dipole. Then the behaviors of these cross-sections under different conditions, such as the thermodynamic phase and the geometric size, are well studied. Also they are compared with those under different theories, such as Rayleigh and Mie theory. The results show that: (1) comparing with Rayleigh approximation, in dipole theory, since there exists higher-order minute items, which include q, the scale factor (SF), and m, the complex refractivity index, in those expressions, all of cross-sections of scattering field change in corporation with the properties of the variation of particle scale and phases. Only if the scale of particles is very small, these changes are not significant. That is to say, to very small particles, results under these two theories have little difference. However, under the dipole theory, those so-called minute items play a significant role when the particle size increases and the phase changes. (2) It is difficult to simply summarize these changes. In some conditions they are good but in others they are bad. It is better to deal with every possibility, respectively.

Keywords: Dipole; Microwave; Precipitation radar

1. Introduction

Nowadays, the band range of conventional weather radar is from 3 to 10 cm. It has been proved that, in a certain range of wave band, much of the interaction between precipitation particles and

☆ This work is supported by National Natural Science Foundation of China (No. 49794030).
* Corresponding author.
E-mail address: simon@ccermail.net (X. Jin).

0022-4073/04/$ - see front matter © 2003 Elsevier Ltd. All rights reserved.
doi:10.1016/S0022-4073(03)00109-2

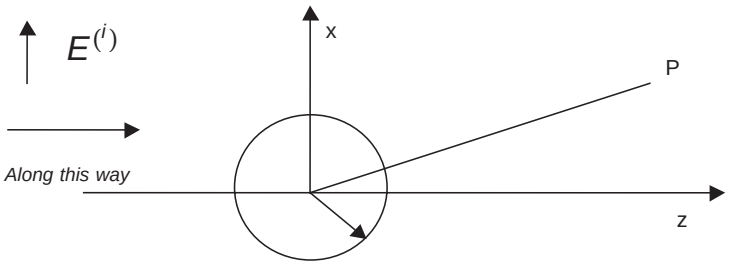

Fig. 1. Demonstration of the model.

radar wave can be described by Rayleigh theory as most particles are too small to be considered the influence of shape. Mason [1], Martinez [2] and Willis [3] have already pointed out by field experiments data that the diameters of most of the raindrops range from 0.1 to 6 mm. According to Rayleigh theory, the influence of the geometric shape of those hydrometeors is neglectable, i.e., they are taken as spots. In fact, the most widely used equation of precipitation retrieving by radar, $Z = aI^b$, which is well known as Z–I relationship, in which, Z represents the radar refractivity factor, I represents the rainfall intensity, a and b are coefficients, is also based on Rayleigh approximation [4]. However, because Rayleigh assumption is too simple, it is not suitable to those particles owning rather large sizes. The scattering theory of small elliptical precipitation particles advocated by Gans solve the scattering problems of non-spherical particles to some extent, the assumption of this theory is to consider precipitation particles as dipoles distributed along three rotary axes. This assumption, in its nature, has a little advantage comparing with Rayleigh approximation because the particle size is not neglectable in this condition. It can be proved (in the next part of this paper) that, when a dipole degenerates into a small spherical particle, the result of this theory is similar as Rayleigh approximation but has an extra minute item. That is to say, when the size of a spherical hydrometeor is not very small comparing with radar wave, it is possible to use this assumption to study the characteristics of scattering field. Thus, in this study, we will study the characteristics of all those cross-sections in that condition and compare them with Mie theory and Rayleigh approximation. To radar with shorter wavelength (such as Ku band), this study is doubtlessly of some meaning. The work band of precipitation radar (PR) loaded on tropical rainfall measurement mission (TRMM) satellite, which was launched in 1997, is about 2.1 cm, which is in Ku band, and is rather shorter than most conventional C band weather radar (such as WS88D). The virtue of this option is high spatial resolution; the attenuation of radar signal is also much severe [5], however. Another tough problem is that the relationship between Z and I is more unstable. In addition, all algorithms to revise PR signal are based on the interaction between electromagnetic wave and precipitation particles [6]. So, in this study, we will discuss quantitative relationship of them in detail beginning with Mie theory.

2. Methods of equations

In Fig. 1, to the diffraction of a single spherical conductor, consider incident wave $\lambda^{(I)}$ is a normalized plane monochromatic wave, if the complex refractivity index (CRI) of the sphere to its

surrounding media (atmosphere) is m, the attenuation cross-section $Q^{(e)}$ and scattering cross-section $Q^{(s)}$ of Mie scattering are [7]

$$Q^{(e)} = \frac{\lambda^{(I)2}}{2\pi} \mathrm{Re} \sum_{l=1}^{\infty} (2l+1)[a_l + b_l], \tag{1}$$

$$Q^{(s)} = \frac{\lambda^{(I)2}}{2\pi} \sum_{l=1}^{\infty} (2l+1)[|a_l|^2 + |b_l|^2]. \tag{2}$$

The backscattering cross-section $Q^{(b)}$ is

$$Q^{(b)} = \frac{\lambda^{(I)2}}{4\pi} \left| \sum_{l=1}^{\infty} (-1)^l (2l+1)(a_l - b_l) \right|^2, \tag{3}$$

where a_l and b_l are coefficients of scattering field. Non-dimensional variable q, which is used to describe the relative scale between the sphere and the incident wavelength, is

$$q = \frac{2\pi}{\lambda^{(I)}} a. \tag{4}$$

In the past several decades, observational data all over the world show that, diameter of rainfall particle ranges from 0.1 to 6 mm while Ku-band ranges from 1.7 to 2.4 cm. As we can see, the difference between them is evident. To most precipitable particles, q is much less than 1. Keeping m^2 as a finite value, if l is 1, it can be proved that [8]

$$a_1 = \frac{2}{3} q^3 \frac{m^2 - 1}{m^2 + 2}$$

$$b_1 = \frac{2}{3} q^5 \frac{m^2 - 1}{30}, \tag{5}$$

thus, we convert (1)–(3) into

$$Q^{(s)} = \frac{3\lambda^2}{2\pi} \{|a_1|^2 + |b_1|^2\} = \frac{128\pi^5}{3\lambda^4} a^6 \left| \frac{m^2 - 1}{m^2 + 2} \right| \left\{ 1 + \left| \frac{q^2}{30} (m^2 + 2) \right|^2 \right\}, \tag{6}$$

$$Q^{(e)} = \frac{3\lambda^2}{2\pi} \mathrm{Re}\{a_1 + b_1\} = \frac{8\pi^2}{\lambda} a^3 \, \mathrm{Im} \left\{ -\frac{m^2 - 1}{m^2 + 2} - q^2 \frac{m^2 - 1}{30} \right\}, \tag{7}$$

$$Q^{(b)} = \frac{\lambda^{(I)2}}{\pi} \left| q^3 \frac{m^2 - 1}{m^2 + 2} - q^5 \frac{m^2 - 1}{30} \right|^2. \tag{8}$$

Obviously, the absorption cross-section is

$$Q^{(a)} = Q^{(e)} - Q^{(s)} = \frac{3\lambda^2}{2\pi} \{\mathrm{Re}\{a_1 + b_1\} - \{|a_1|^2 + |b_1|^2\}\}. \tag{9}$$

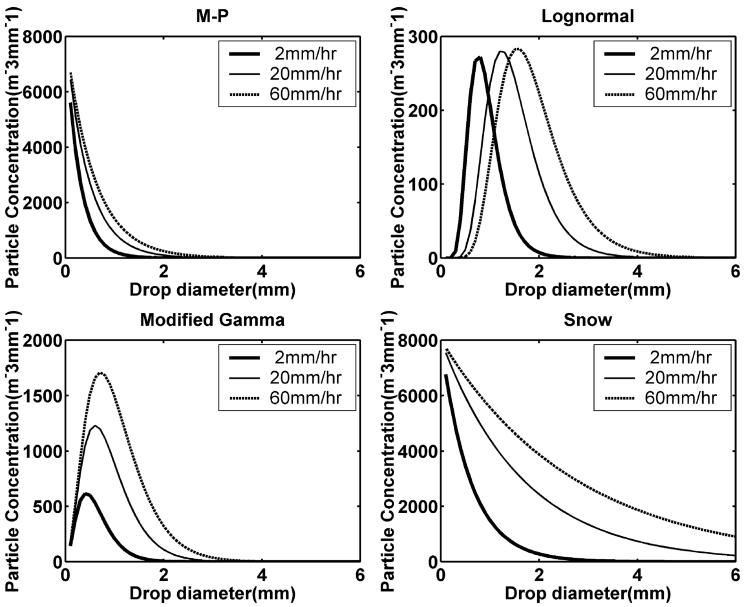

Fig. 2. Four kinds of RSD ([10–12]).

Use the condition of Rayleigh approximation $|mq| \ll 1$, if we ignore those minute terms, the formulas of scattering field are

$$Q^{(s)} = \frac{128\pi^5}{3\lambda^4} a^6 \left| \frac{m^2-1}{m^2+2} \right|, \tag{10}$$

$$Q^{(b)} = \frac{64\pi^5}{\lambda^4} a^6 \left| \frac{m^2-1}{m^2+2} \right|^2, \tag{11}$$

$$Q^{(a)} = \frac{8\pi^2}{\lambda} a^3 \operatorname{Im}\left\{ -\frac{m^2-1}{m^2+2} \right\}, \tag{12}$$

$$Q^{(e)} = Q^{(a)} + Q^{(s)} = \frac{8\pi^2}{\lambda} a^3 \operatorname{Im}\left\{ -\frac{m^2-1}{m^2+2} \right\} + \frac{128\pi^5}{3\lambda^4} a^6 \left| \frac{m^2-1}{m^2+2} \right|. \tag{13}$$

Now, the problem is that, comparing with most weather radar, the wavelength of TRMM/PR is 2.1 cm, a bit short. In Fig. 2, the results of several widely used raindrop size distribution (RSD), such as M–P distribution, gamma distribution, lognormal distribution, snow distribution, show that, the average diameter and median diameter of precipitation particles increase with the increase of precipitation intensity, thus, the number of precipitation particles fitting to the condition $q \ll 1$ decreases. If we still use Rayleigh approximation, what is the error when we convert (6)–(9) to (10)–(13)? Based on the work of Battan [9], we know that, when $q < 0.13$, the result of Rayleigh theory is almost same as that of Mie theory. To PR, which works in Ku band, it is easy to draw the conclusion that the diameter of precipitation particles is less than 0.84 mm. However, as the intensity of precipitation increases, more and more percent of precipitation particles go beyond the limitation (see Fig. 2).

Obviously, because of the term q indicating the scale in (6)–(9), which we call dipole approximation in this study, are stricter than Rayleigh approximation. What is the feasible range of application for these formulas? We will discuss it in detail in the following.

3. Discussions

We will compare the ratio $Q^{(m)}/Q^{(d)}$ (show as solid line) of these cross-sections under dipole approximation to cross-sections under Mie theory with the ratio $Q^{(m)}/Q^{(r)}$ (shown as dot line) of cross-sections under complete Rayleigh approximation to cross-sections under Mie theory. We use algorithms advocated by Bohren and Huffman [13] to calculate all the cross-sections under Mie theory. We set wavelength 2.1 cm, and there are 3 kinds of precipitation particles: liquid water, ice and soft hail (shown as red, green, blue line, separately, and the mixing ratio of ice to liquid water in soft hail is 1:1). And the composition mode is advocated by Debye [14], the temperature is 273 K. The abscissa is the non-dimensional variable q, and since the upper limit of the diameter of precipitation particles is 6 mm, the maximum of q is about 0.9; the ordinate is the ratio which is also non-dimensional variable of these cross-sections. In this study, if the ratio is between 0.9 and 1.1 (the region between the two black plus line in the following figures), it means that the error is acceptable.

3.1. Scattering cross-section

Fig. 3 shows how the ratio of scattering cross-sections varies with q. The range of q in left figure is from 0.015 to 0.9, while in right figure is from 0.015 to 0.4. From Fig. 3, we can see:

(1) The $Q^{(s)}$ of spherical ice particles is the most stable, and the results of the two calculation methods are almost same. Although the ratio increases with the increase of scale of particles, it lies between 1 and 1.1. This is easy to explain. Since m_i, the CRI of spherical ice particle, is much less than m_w, that of liquid water particles, the last term in (6) is very small, thus, the result of dipole assumption is almost same as the result of Rayleigh assumption in a large range.

(2) Compared with spherical ice particles, $Q^{(s)}$ of liquid water particles is unstable. The two methods show the same trend: when q is very small, the ratio is close to 1; while q increases, the ratio increases first and decreases then, which indicates that the $Q^{(s)}$ of the two methods is less than that of Mie theory firstly and larger than that of it then. The difference is that, the $Q^{(s)}$ of dipole assumption is larger than that of Rayleigh assumption, which makes the upper limit which satisfies the condition of error, of diameter of liquid water particles less than that of Rayleigh theory. The reason is that, although the term containing q in (6) is very small, it is positive, and this term increases very quickly while it is neglected as a minute term in (10). The results above show that dipole assumption is much stricter than Rayleigh theory.

(3) To soft hail, if q is less than 0.7, the curves lie between the lines of pure spherical ice particles and liquid particles. The difference between the two approximation methods is less than that of pure water, and is greater than that of pure ice; if q is larger than 0.7, the curves exhale.

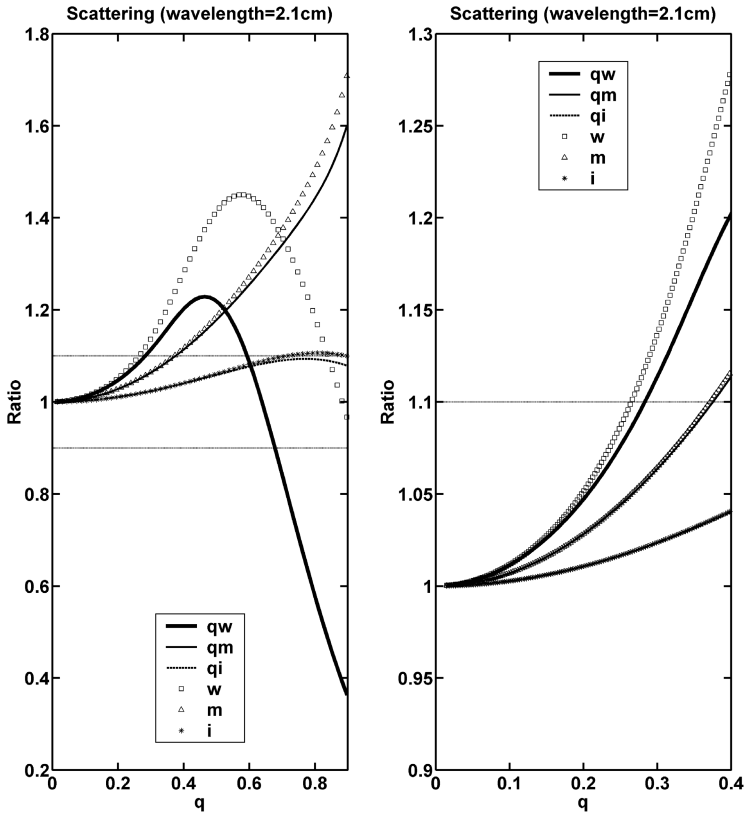

Fig. 3. Relationships between the ratios of scattering cross-sections under dipole and Rayleigh assumptions to Mie theory separately and q (the former three lines in the legend represent the former assumption and the rest represent the later; w, i and m represent liquid, solid and soft hail, separately; the right one is same as the left but the limitation of q is up to 0.4)

From that trend, we can see that if the ratio of ice increases, the behavior tends to be pure ice particles and if the ratio of water increases, it performs similar with pure water particles.

3.2. Backscattering cross-section

Fig. 4 describes how backscattering cross-sections $Q^{(b)}$ (radar cross-sections) change while q increases. From this figure, we can see:

(a) In spite of the thermodynamic phase of precipitation particles, the difference of $Q^{(b)}$ calculated though the two formulas is sensitive to q, the scale factor, which makes that although q is very small, the difference is striking. In addition, in the range of this figure, no matter how q and phase change, the $Q^{(b)}$ under dipole approximation is always less than that under Rayleigh approximation.
(b) Relatively, $Q^{(b)}$ of spherical ice particles are the most stable, especially, under dipole approximation, when q is between 0.015 and 0.6, the result of this method is almost same as that of Mie

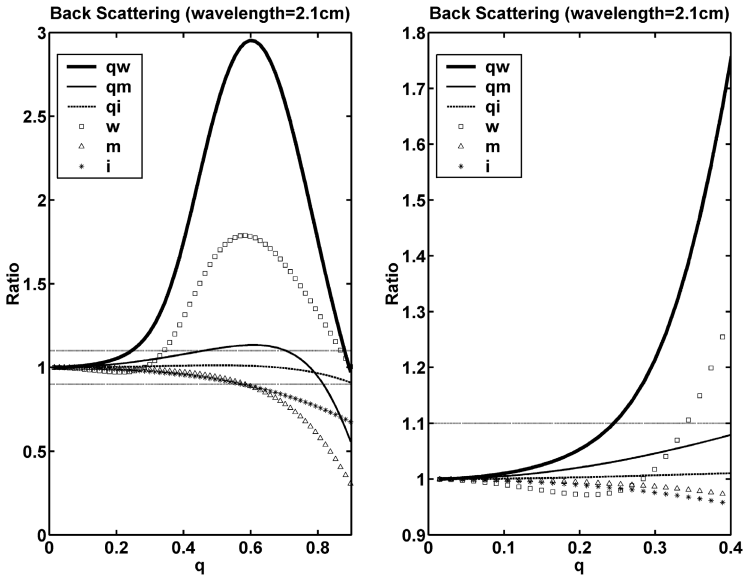

Fig. 4. Same as Fig. 3 but for backscattering cross-sections.

Theory. When q is larger than 0.6, the ratio decreases a little, but always lies between 0.9 and 1. However, we note that, if q is equal to 0.5, the ratio of the result of Rayleigh approximation to that of Mie theory is already below 0.9.

(c) $Q^{(b)}$ of liquid particles change greatly while q changes. When q is between 0.3 and 0.9, the ratio is above 1, increasing firstly and decreasing then, and goes to the peak when q is about 0.6. This indicates that, in this range, the $Q^{(b)}$ calculated by these two methods are less than that by Mie theory, and the minimum appears when q is about 0.6. Additionally, from the right figure, we can see that, if q is below 0.08, the results by the two methods are almost same as that by Mie theory; if q is between 0.08 and 0.3, $Q^{(b)}$ of dipole approximation is less than that of Mie theory, while $Q^{(b)}$ of Rayleigh approximation is greater than that of Mie theory.

(d) Results of particles composed by soft hail are between that of pure liquid particles and ice particles. If q is below 0.1, the results are almost same as that of Mie theory; as q increases, $Q^{(b)}$ of Rayleigh theory exceeds that of Mie theory, and the ratio goes beyond 0.9 when q is about 0.6. As for the $Q^{(b)}$ by dipole approximation, from the condition that is q equal to 0.1, the ratio increases firstly and decreases then as q increases. When q is equal to 0.75, the ratio begins to small than 1, which indicates that $Q^{(b)}$ of dipole approximation begins to be greater than that of Mie theory.

As we know, the $Q^{(b)}$ is of great physical importance since it is the theoretical basis of radar sounding. From what have been discussed above, the $Q^{(b)}$ is strongly influenced by scale and phase, especially by CRI of liquid particles. So, the theoretical radar refractivity index that can be applied has a limited range. However, as for ice particles and particles mixed with a large proportion of ice, the $Q^{(b)}$ of dipole approximation has a greater application range than that of Rayleigh approximation. Thus, to TRMM/PR, at least in theory, the dipole approximation formula is possibly more suitable

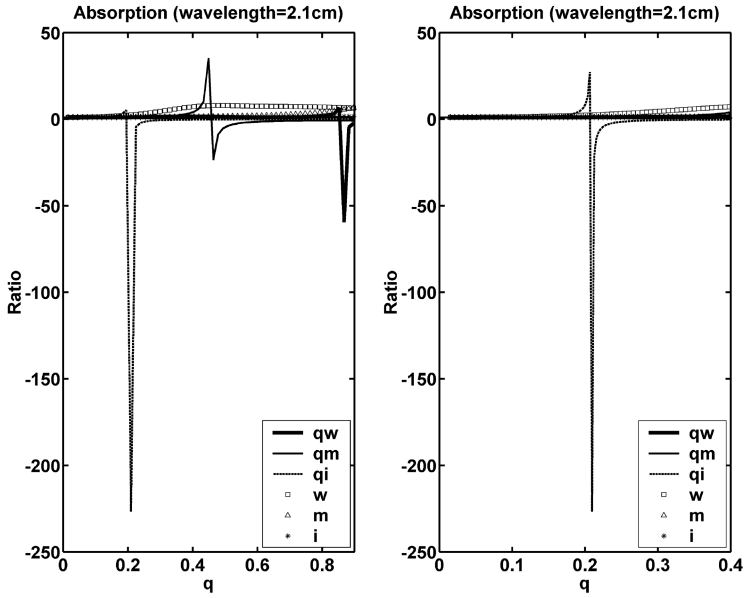

Fig. 5. Same as Fig. 3 but for absorption cross-sections.

to precipitation echo in ice layer and the layer mixed by ice and water (mixed in the way advocated by Debye) above 0°C layer.

3.3. Absorption cross-section

Fig. 5 describes how the ratio of $Q^{(a)}$ change while scale factor q changes. Note that, (9) is deducted though the law of energetic conservation indirectly. With the change of scale and phase, the two finite terms containing q and m will influence the results unpredictably. From the figure above, we can see:

(1) For ice particles, because of the influence of the two finite terms, the ratio of dipole approximation jumps when q is between 0.2 and 0.21, from a positive value which increases quickly to a negative one, and keeps as a negative value later. Obviously, this results are not reasonable. When q is below 0.09, the ratio of $Q^{(a)}$ of Mie theory to that of dipole approximation is above 1.0 and below 1.1, which indicates that although the result of dipole approximation is less than that of Mie theory in this range, it is very close to the latter. So, the application range of dipole approximation is very limited.
(2) As to the other two cases, distribution of the curve under dipole approximation resembles that of ice particles. In correspondence, the application range of this approximation is that q is below 0.68 for pure liquid particles, and below 0.17 for particles composed of liquid and ice water. The trend is that the application range increases while the proportion of liquid water increases.
(3) The application range of Rayleigh approximation is little broader than that of dipole approximation, so is the stability—there is no jump in the region of Fig. 5. Of course, we cannot prove that Rayleigh approximation is more acceptable according to the formula, because the condition

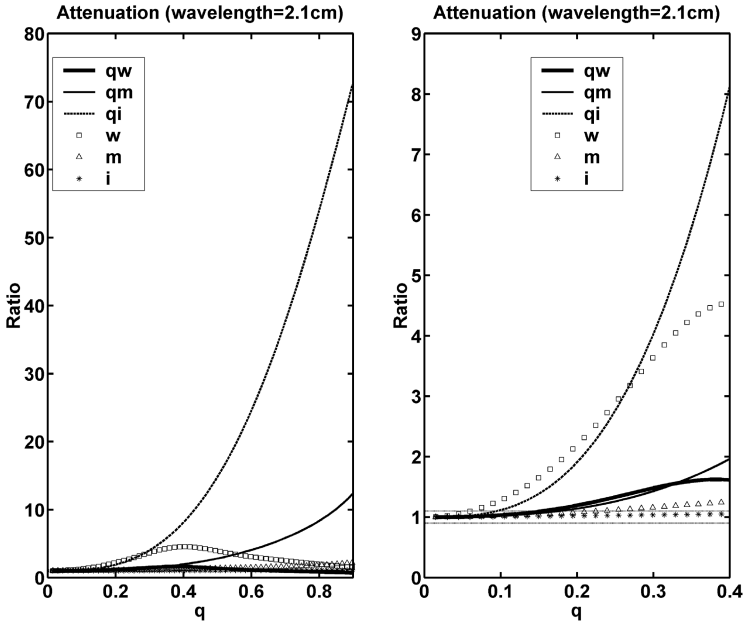

Fig. 6. Same as Fig. 3 but for attenuation cross-sections.

of Rayleigh approximation is not so strict, and ignores the effects of finite terms which have close relationship with scale factor, thus, the $Q^{(a)}$ under this assumption is not sensitive to scale factor. In fact, from this figure we can see that, in spite of the change of phase of particles, in application range of dipole approximation, the $Q^{(a)}$ of dipole approximation is much closer to that of Mie theory than that of Rayleigh approximation.

3.4. Attenuation cross-section

Fig. 6 describes how cross-sections of liquid water $Q^{(e)}$ changes while q changes. Fig. 7 is about liquid water (13) shows that, under the condition of Rayleigh approximation, comparing with $Q^{(e)}$, $Q^{(s)}$ is very small, that's why $Q^{(a)}$ of Rayleigh approximation in Fig. 6 resemble those in Fig. 5, while that of dipole approximation has evident difference. From the two figures above, we can see:

(1) Under the condition of dipole approximation, no matter how q changes, in such region (Fig. 6), attenuation of Mie theory and the ratio of attenuation of ice particles to particles mixed by ice and water increases consistently, which indicates that, as scale factor increases, the approximate $Q^{(e)}$ is smaller and smaller than true $Q^{(e)}$, and the trend of ice particles is the most evident. While that of pure liquid particles is not sensitive to scale factor. When q is smaller than 0.16, the ratio is consistently below 1.1, and it increases a little then, but when q is above 0.4, it begins to decrease. When q is above 0.8, it begins to be smaller than 0.9.
(2) Comparing with dipole approximation, $Q^{(e)}$ of pure liquid particles under Rayleigh approximation is much less than that of the former, which is shown in Fig. 7. That is to say, the ratio is always larger than that of dipole approximation. This indicates that, to pure liquid particles, dipole approximation is closer to Mie theory, so it has a larger application range.

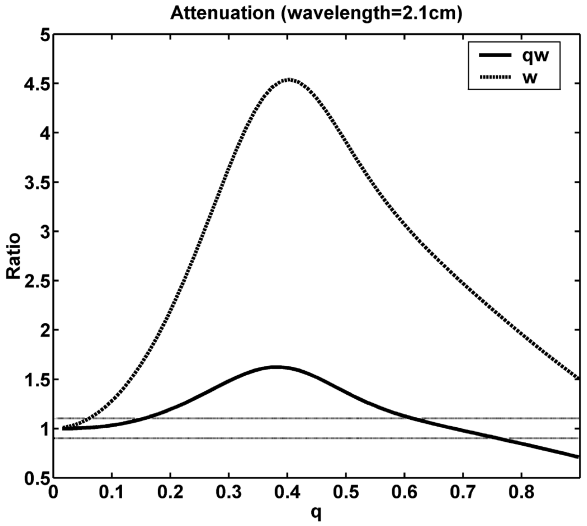

Fig. 7. Same as Fig. 3 but is only for attenuation.

(3) In the two cases containing ice, $Q^{(e)}$ under dipole approximation is always more unstable than that under Rayleigh theory, which indicates that CRI of ice has a rather important effect on the $Q^{(e)}$ of the dipole approximation.

4. Conclusions

From what have been discussed above, we can draw these conclusions:

(1) Since a high order minute term under dipole approximation containing scale factor and complex refractivity index, comparing with Rayleigh approximation, the characteristics of all the cross-sections of scattering field change to a certain content while particles size and phase change; only when the scale of particles is quite small, these difference are not evident, that's to say, to very small particles, the two approximate methods have little difference.
(2) The behavior of all cross-sections caused by scale and phase is not same, and it is hard to summarize by a simple rule. So we should use different methods to deal with different circumstances.

References

[1] Mason BJ. The physics of clouds. Oxford: Oxford University Press, 1971.
[2] Martinez D, Gori EG. Raindrop size distributions in convective clouds over Cuba. Atmos Res 1999;52:221–39.
[3] Willis PT. Functional fits to some observed drop size distributions and parameterization of rain. J Atmos Sci 1984;41(9):1648–61.
[4] Zhang PC. Radar meteorology. Beijing: Meteorology Press, 1988.
[5] Meneghini R, et al. The TRMM precipitation radar: opportunities and challenges. 29th International Conference on Radar Meteorology, Montreal, 12–16 July 1999. p. 751–3.

[6] Marzoug M, Amayenc P. Improved range-profiling algorithm of rainfall rate from a space-borne radar with path-integrated attenuation constraint. IEEE Trans Geosci Remote Sensing 1991;29(4):584–92.
[7] Liou K. An introduction to atmospheric radiation. New York: Academic Press, 1980.
[8] Born M, Wolf E. Principles of optics. Oxford: Pergamon Press, 1959.
[9] Battan LJ. Radar observation of the atmosphere. Chicago, IL: The University of Chicago Press, 1973.
[10] Bohren CF, Huffman DR. Absorption and scattering of light by small particles. New York: Wiley, 1983.
[11] Marshall JS, Palmer WM. The distribution of raindrops with size. J Meteorol 1948;5:165–6.
[12] Sekhon RS, Srivastava RC. Snow size spectra and radar reflectivity. J Atmos Sci 1970;27:983–94.
[13] Ulbrich CW. Natural variations in the analytical form of the raindrop size distribution. J Appl Meteorol 1983;22: 1764–75.
[14] Debye P. Polar molecules. New York: Chemical Catalogue Co, 1929.